Published in final edited form as:

J Am Chem Soc. 2020 July 15; 142(28): 11978–11982. doi:10.1021/jacs.0c04023.

A stable ferryl porphyrin at the active site of Y463M BthA

Kimberly Rizzolo[1,‡], **Andrew C. Weitz**[1,2,‡], **Steven E. Cohen**[3], **Catherine L. Drennan**[3,4,5], **Michael P. Hendrich**[2], **Sean J. Elliott**[1,*]

[1]Boston University, Dept. of Chemistry, Boston, MA 02215

[2]Carnegie Mellon University, Dept. of Chemistry, Pittsburgh, PA 15213

[3]Massachusetts Institute of Technology, Dept. of Chemistry, Cambridge, MA 02139

[4]Massachusetts Institute of Technology, Dept. of Biology, Cambridge, MA 02139

[5]Howard Hughes Medical Institute, Cambridge, MA 02139

Abstract

BthA is a diheme enzyme that is a member of the bacterial cytochrome c peroxidase superfamily, capable of generating a highly unusual Fe(IV)Fe(IV)=O oxidation state, known to be responsible for long-range oxidative chemistry in the enzyme MauG. Here we show that installing a canonical Met ligand in lieu of the Tyr found at the heme of MauG associated with electron transfer, results in a construct that yields an unusually stable Fe(IV)=O porphyrin at the peroxidatic heme. This state is spontaneously formed at ambient conditions using either molecular O_2 or H_2O_2. The resulting data illustrate how a ferryl iron, with unforeseen stability, may be achieved in biology.

Graphical Abstract

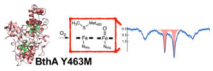

Recently we have reported the diheme enzyme from *Burkholderia* named BthA,[1] a new member of the bacterial cytochrome *c* peroxidase (bCCP) superfamily, that encompasses canonical periplasmic enzymes responsible for the removal of reactive oxygen species such as hydrogen peroxide (H_2O_2) in many Gram negative bacteria,[2–3] as well as enzymes YhjA, which uses H_2O_2 as a terminal electron acceptor,[4] and MauG, responsible for biosynthesis of tryptophan tryptophyl quinone (TTQ), the cofactor of methylamine dehydrogenase (MADH). [5–8] Although all members of the bCCP family are predicted to have a 5-coordinate (5c), *c*-type heme site responsible for binding H_2O_2, they display diversity with respect to a second, six-coordinate (6c) heme associated with electron transfer (ET). The 6c

* ***Corresponding Author*** elliott@bu.edu .

‡Author Contributions

These authors contributed equally.

No competing financial interests have been declared.

ASSOCIATED CONTENT

Supporting Information.

The Supporting Information is available free of charge on the ACS Publications website at https://doi.org/10.1021/jacs.0c04023. It includes experimental procedures, spectroscopic data, and crystallographic data collection and refinement statistics (PDF).

heme in MauG, possesses Tyr-His ligation, whereas other bCCPs typically possess Met-His (Figure 1A). The difference in coordinating ligands has been linked to variation in the redox potentials of the hemes for bCCPs and MauG[9], and is suggested to be a key to achieving the H_2O_2 induced formation of a *bis*- Fe(IV)Fe(IV)=O state of MauG.[10–12] We have shown that *Burkholderia* BthA possesses the same Tyr-His ligation at the 6c heme, and generates the same reported *bis*-Fe(IV)Fe(IV)=O species. [1]

Here we find that upon mutating the ligating Tyr463 of BthA to the cognate Met ligand found in bCCPs, Met463 binding to the Fe of heme 6c does not occur, and in the purified enzyme a stable Fe(IV)=O species is present at the 5c active site >20 Å away from the site of the substitution.

We predicted that generation of the BthA Y463M variant would transform the redox properties of the 6c heme of BthA significantly. In canonical bCCPs, the role of the 6c heme is predicted to be associated with ET, relaying reducing equivalents to the peroxidatic 5c active site heme.[13–17] The Met-His coordination of the 6c heme is tuned to relatively high redox potentials (>+250 mV vs. SHE)[18–20] which stabilize a semi-reduced state (i.e., $Fe^{II}_{6c}Fe^{III}_{5c}$).[19–21] In MauG, a Tyr-His ligation at the 6c heme causes a decrease in reduction potentials for both hemes (−159 mV vs. SHE and −244 mV vs. SHE)[22], such that a stable semi-reduced redox state cannot be obtained. Mutation of the Tyr ligand of MauG to either Met[23] or His[9] completely disrupts the ability of MauG to oxidize the preMADH substrate.

Upon generation of the Y463M mutant of BthA, physical characterization demonstrated immediately that Y463M is not like typical bCCPs. Upon treatment with ascorbate, the variant does not optically adopt a semi-reduced state as has been reported for canonical bCCPs, indicated by the presence of reduced Q-bands [19, 24] (Figure 1B). Direct electrochemistry of Y463M shows voltammetric features of the protein similar to wild-type (WT) BthA and MauG, and a discernible higher potential signature (Figure 1C). Deconvolution of the voltammetry gave redox couples of −78 mV and −159 mV, indicating both heme sites shifted more positive in potentials compared to WT (−121 mV and −165 mV, all potentials vs. SHE).[1] Although dye-linked peroxidase activity assays showed the Y463M variant was capable of catalytically reducing H_2O_2 to water, with K_m and k_{cat} values comparable to WT (3.3 ± 0.4 μM and 6.4 ± 0.8 s^{-1}, respectively), addition of peroxide to the as-isolated diferric state of Y463M did not show evidence of the *bis*-Fe(IV) state when analyzed by near Infra-Red (NIR) spectroscopy. WT BthA and MauG react with peroxide to form the *bis*-Fe(IV) intermediate, which can be monitored through the generation of a NIR feature at 950 nm, along with a shift in the Soret and appearance of charge transfer bands.[11] Upon treatment with H_2O_2, Y463M shows none of these traits (Figure 1D). Thus, these data appeared in conflict: the optical and kinetic data indicted a canonical bCCP-like behavior, yet the lack of a significant shift in redox potential suggest the changes observed in the mutant are not dependent on the redox potential of the 6c heme in BthA.

The X-ray crystal structure of Y463M was solved to 1.59 Å resolution, and the structure confirms that the 6c heme environment was not as anticipated. Although the overall fold is the same as WT (rmsd = 0.309 Å over all atoms) and the substituted Met463 residue is

present based on the electron density, the sulfur of Met463 is too far (~4Å) to coordinate the heme Fe (Figure 2). The side chain of Tyr is longer than the side chain of Met, and without any backbone movement, Met463 simply cannot reach the heme Fe.

The five-coordinate nature of both hemes of Y463M BthA was further examined spectroscopically to provide additional insight into the unexpected crystallographic results. The EPR spectra for aerobically-purified Y463M BthA indicated a strong high spin Fe(III) signal (HS, S = 5/2) present in the sample (Figure S1), with no evidence of low spin (LS, S = 1/2) signal attributed to the 6c heme in WT.[1] The high spin signal near $g = 6$ represents a mixture of two species, one axial (E/D = 0) like the 5c peroxidatic heme in WT, and one having higher anisotropy (E/D = 0.02) than the 5c peroxidatic heme in WT. The simulations of Figure S1 indicate species percentages of 20% (0.22 mM) and 33% (0.36 mM), respectively, relative to the total protein amount (1.1 mM). Quantification of the heme content by Electronic Absorption revealed full heme occupancy, suggesting the missing iron was due to the presence of EPR-silent species in this sample.

Mössbauer spectra of WT BthA (Figure 3A) showed LS and HS Fe(III) hemes in equal amounts, consistent with previous work.[1,10] The species contributing to the simulation of the data are displayed above Figure 3A (see Table S2 for fit parameters[25]). In contrast, the Mössbauer spectra of Y463M BthA (Figure 3B) showed two HS Fe(III) species (dotted trace 27%, dashed trace 41% of iron) and no LS Fe(III) heme, consistent with the amounts of axial (E/D = 0) and anisotropic (E/D = 0.02) species, respectively, detected by EPR in Figure S1. Y463M BthA showed an additional species displaying a doublet (Figure 3B, red fill, 33% of iron). Although the aerobic as-isolated sample had not been exposed to H_2O_2, the parameters of the doublet ($\delta = 0.08$ mm/s, $\Delta E_Q = 1.67$ mm/s) matched the Fe(IV)=O species of the peroxidatic heme found in WT after H_2O_2 addition. The presence and relative amount of Fe(IV)=O in as-isolated Y463M was reproducible across three independent preparations of ^{57}Fe-enriched Y463M, that had been expressed recombinantly in *E. coli*, and purified aerobically. The amounts of the species indicate that the WT LS heme converts into the anisotropic (E/D=0.02) HS heme, whereas the WT HS axial (E/D = 0) heme is partially converted to the Fe(IV)=O species in Y653M BthA. Thus, the new Fe(IV)=O species found in Y463M BthA is associated with the peroxidatic heme.

To test that the air-oxidized species containing the Fe(IV)=O is still active with respect to potential hydrogen peroxide reactivity (and not an inactive byproduct from purification), we reacted the as-isolated Y463M BthA sample with reductant. Addition of excess ascorbate resulted in complete loss of the Fe(IV) doublet (Figure 3C), and formation of the axial HS heme associated with the peroxidatic heme (now ~47% of total Fe). The simulation in Figure 3C also uses the rhombic HS species in approximately equal amounts as in Figure 3B (41%). Unaccounted area in this fit (~12%) could conceivably be assigned to residual Fe(IV)O, but the noise in the data preempts a conclusive assignment. Ascorbate did not reduce either heme to Fe(II), consistent with the measured redox potentials of the hemes (Figure 1C). EPR experiments confirmed that reduction caused growth of only the axial HS Fe(III) species associated with the peroxidatic heme in WT (Figure S1). Likewise, electronic absorption spectroscopy indicated that addition of sodium ascorbate resulted in growth of a feature at 625 nm and narrowing of the Soret band which is likely associated with Fe(III)

heme formation. Subsequent addition of excess H_2O_2 to the reduced sample generated the same Fe(IV)=O heme species in similar yield to the as-isolated sample (Figure 3D). The HS Fe(III) species associated with the peroxidatic heme in Figure 3C was lost upon peroxide treatment in Figure 3D.

To address if ambient O_2 was the source of the spectroscopically observed Fe(IV)=O in as-isolated Y463M BthA, we purified the variant under strict anaerobic conditions. The Mössbauer spectrum (Figure 4A) showed three doublets: two doublets associated with Fe(II) (δ_1 = 0.89, ΔE_{Q1} = 2.22 mm/s, 42% of Fe; δ_2 = 0.91, ΔE_{Q2} = 1.65 mm/s, 27% of Fe, blue fill), and a third corresponding to Fe(II)-CO[26] (δ = 0.25, ΔE_Q = 0.49 mm/s, 23% of Fe, green fill). The broad underlying feature was from a minor adventitious paramagnetic species. The Fe(II)-CO species and adventitious iron may be from CO generated in the decay of heme species during lysis (and optical data (Figure S2) verified its presence in anaerobic preparations of Y463M). The doublet associated with Fe(IV)=O was not present. Taking the anaerobic sample (Figure 4A) and exposing it to O_2 for 10 min (Figure 4B), the Fe(II)-CO species was unchanged (28% of Fe), the two Fe(II) species were replaced by a mixture of oxy-heme[26] (δ = 0.27, ΔE_Q = 2.41 mm/s, 21% of Fe, orange fill), and HS Fe(III) heme (broad underlying magnetic species, 31%), and importantly, the Fe(IV)=O species observed in aerobically-purified Y463M form (20%, red fill). The black line on Figure 4B shows the resulting simulated sum for all species. Thus, the Fe(IV)=O species is O_2-dependent, generated at the peroxidatic heme site, and is not generated by reaction of the enzyme with endogenous peroxide contamination during purification.

At this time, the exact mechanism of O_2 reactivity to form the Fe(IV)=O species at the peroxidatic heme of Y463M, and an explanation for its long lifetime in the aerobically purified samples, are both unclear. However, the presence of oxy-heme as detected by Mössbauer (Figure 4B) suggests O_2 binding to the peroxidatic heme and subsequent activation to a Fe(IV)=O complex. As noted above, the Fe(IV)=O can also be generated when the diferric Y463M variant reacts with H_2O_2 (Figure 3D). In the related case of the Y294H variant of MauG[9, 27], installation of His at the same position as Y463 (BthA numbering) lead to the formation of a Compound-I like state upon peroxide addition (Cpd-I, Fe(IV)=O $R^{+\bullet}$), similar to the proposed mechanism for diheme peroxidase NeCCP[28]. (Reactivity with O_2 appears unique to Y463M BthA.) Despite formation of a Cpd-I species, the Y294H MauG variant had a decreased reactivity towards preMADH, demonstrating Tyr294 plays a crucial role in forming the *bis*-Fe(IV) species that is specifically required for TTQ biosynthesis. [9] In addition, the Cpd-I state of Y294H MauG was about as kinetically stable as that of the WT bis-Fe(IV) state – where decay back to a diferric resting state was achieved over 5–10 minutes. Therefore, in MauG, the substitution of 6c heme ligands prohibit formation of the *bis*-Fe(IV) species, but do not necessarily limit the 5c heme from achieving high valent oxidation states.

In contrast, exposure to O_2 in the Y463M BthA variant can activate the Fe(II) peroxidatic heme alone to form a stable Fe(IV)=O state, and the lack of Tyr463 apparently impacts how the active site heme may relax back to a resting state, allowing the Fe(IV)=O to persist for days, instead of minutes. Despite this long time scale, we were unable to detect the Fe(IV)=O species crystallographically (Figure S7) as data-quality crystals of this

BthA variant protein took weeks, not days, to grow (see methods). The long lifetime of this species may suggest that electron transfer into and out the BthA peroxidatic heme is fundamentally slower, and/or the latent oxidizing power of the BthA ferryl is weaker than that found in MauG. Regardless, whereas the highly oxidized states of MauG/variants relax to a resting state in minutes, here the Fe(IV)=O of BthA Y463M is stable for days.

As shown here, BthA poses a rich system for exploring how ET is mediated within the protein scaffold. By generating mutations of key residues identified to play a role in the reactivity of bCCPs and MauG, we have revealed that mutation of Tyr463 to mimic the canonical Met-His ligation of a bCCPs results in an Fe(IV)=O species at the peroxidatic 5c heme site with benchtop stability. There is much to learn yet regarding what tunes the reactivity of BthA and other bCCP and MauG orthologs that might bind O_2. Further, the presence of such a long-lived ferryl species makes the Y463M variant of BthA a model system for exploring the stability of Fe(IV)=O species and electronic communication of that site with other redox cofactors.

Supplementary Material

Refer to Web version on PubMed Central for supplementary material.

ACKNOWLEDGMENT

This work has been supported by the National Institutes of Health (S.J.E., R01-GM110390, M.P.H., R01-GM077387, C.L.D., R35-GM126982). S.E.C. is supported by NIH T32 GM008334 and The Martin Family Society of Fellows for Sustainability. C.L.D. is a Howard Hughes Medical Investigator, and is a Senior Fellow of the Bio-inspired Solar Energy Program, Canadian Institute for Advanced Research (CIFAR). This work is based upon research conducted at the Northeastern Collaborative Access Team beamlines, which are funded by NIH (P30 GM124165). The Eiger 16M detector on 24-ID-E is funded by a NIH-ORIP HEI grant (S10OD021527). This research used resources of the Advanced Photon Source, a U.S. Department of Energy (DOE) Office of Science User Facility operated for the DOE Office of Science by Argonne National Laboratory under Contract No. DE-AC02-06CH11357).

REFERENCES

1. Rizzolo K; Cohen SE; Weitz AC; López Muñoz ML; Hendrich MP; Drennan CL; Elliott SJ, A widely distributed diheme enzyme from Burkholderia that displays an atypically stable bis-Fe(IV) state. Nature Communications 2019, 10, 1101.
2. Goodhew CF; Wilson IB; Hunter DJ; Pettigrew GW, The cellular location and specificity of bacterial cytochrome c peroxidases. The Biochemical journal 1990, 271 (3), 707–12. [PubMed: 2173903]
3. Welinder KG, Superfamily of plant, fungal and bacterial peroxidases. Current Opinion in Structural Biology 1992, 2 (3), 388–393.
4. Khademian M; Imlay JA, Escherichia coli cytochrome c peroxidase is a respiratory oxidase that enables the use of hydrogen peroxide as a terminal electron acceptor. Proceedings of the National Academy of Sciences of the United States of America 2017, 114 (33), E6922–E6931. [PubMed: 28696311]
5. Wang Y; Graichen ME; Liu A; Pearson AR; Wilmot CM; Davidson VL, MauG, a novel diheme protein required for tryptophan tryptophylquinone biogenesis. Biochemistry 2003, 42 (24), 7318–25. [PubMed: 12809487]
6. Lee S; Shin S; Li X; Davidson VL, Kinetic mechanism for the initial steps in MauG-dependent tryptophan tryptophylquinone biosynthesis. Biochemistry 2009, 48 (11), 2442–7. [PubMed: 19196017]

7. Shin S; Abu Tarboush N; Davidson VL, Long-range electron transfer reactions between hemes of MauG and different forms of tryptophan tryptophylquinone of methylamine dehydrogenase. Biochemistry 2010, 49 (27), 5810–6. [PubMed: 20540536]
8. Jensen LM; Sanishvili R; Davidson VL; Wilmot CM, In crystallo posttranslational modification within a MauG/pre-methylamine dehydrogenase complex. Science 2010, 327 (5971), 1392–4. [PubMed: 20223990]
9. Abu Tarboush N; Jensen LM; Feng M; Tachikawa H; Wilmot CM; Davidson VL, Functional importance of tyrosine 294 and the catalytic selectivity for the bis-Fe(IV) state of MauG revealed by replacement of this axial heme ligand with histidine. Biochemistry 2010, 49 (45), 9783–91. [PubMed: 20929212]
10. Li X; Fu R; Lee S; Krebs C; Davidson VL; Liu A, A catalytic di-heme bis-Fe(IV) intermediate, alternative to an Fe(IV)=O porphyrin radical. Proceedings of the National Academy of Sciences of the United States of America 2008, 105 (25), 8597–600. [PubMed: 18562294]
11. Geng J; Dornevil K; Davidson VL; Liu A, Tryptophan-mediated charge-resonance stabilization in the bis-Fe(IV) redox state of MauG. Proceedings of the National Academy of Sciences of the United States of America 2013, 110 (24), 9639–44. [PubMed: 23720312]
12. Geng J; Davis I; Liu A, Probing bis-Fe(IV) MauG: experimental evidence for the long-range charge-resonance model. Angewandte Chemie 2015, 54 (12), 3692–6. [PubMed: 25631460]
13. Atack JM; Kelly DJ, Structure, mechanism and physiological roles of bacterial cytochrome c peroxidases. Advances in microbial physiology 2007, 52, 73–106. [PubMed: 17027371]
14. Fulop V; Ridout CJ; Greenwood C; Hajdu J, Crystal structure of the di-haem cytochrome c peroxidase from Pseudomonas aeruginosa. Structure 1995, 3 (11), 1225–33. [PubMed: 8591033]
15. Shimizu H; Schuller DJ; Lanzilotta WN; Sundaramoorthy M; Arciero DM; Hooper AB; Poulos TL, Crystal structure of Nitrosomonas europaea cytochrome c peroxidase and the structural basis for ligand switching in bacterial di-heme peroxidases. Biochemistry 2001, 40 (45), 13483–90. [PubMed: 11695895]
16. Hoffmann M; Seidel J; Einsle O, CcpA from Geobacter sulfurreducens is a basic di-heme cytochrome c peroxidase. Journal of molecular biology 2009, 393 (4), 951–65. [PubMed: 19735665]
17. Nóbrega CS; Pauleta SR, Reduction of hydrogen peroxide in gram negative bacteria — bacterial peroxidases. In Advances in microbial physiology, Poole RK, Ed. Elsevier: London, U.K., 2019; Vol. 47.
18. Gilmour R; Goodhew CF; Pettigrew G; Prazeres S; Moura I; Moura J, Spectroscopic characterization of cytochrome c peroxidase from Paracoccus denitrificans. Biochemical J 1993, 294 (3), 745–752.
19. Arciero DM; Hooper AB, A di-heme cytochrome c peroxidase from Nitrosomonas europaea catalytically active in both the oxidized and half-reduced states. The Journal of biological chemistry 1994, 269 (16), 11878–86. [PubMed: 8163487]
20. Pulcu GS; Frato KE; Gupta R; Hsu HR; Levine GA; Hendrich MP; Elliott SJ, The diheme cytochrome c peroxidase from Shewanella oneidensis requires reductive activation. Biochemistry 2012, 51 (5), 974–85. [PubMed: 22239664]
21. Wolf MW; Rizzolo K; Elliott SJ; Lehnert N, Resonance Raman, Electron Paramagnetic Resonance, and Magnetic Circular Dichroism Spectroscopic Investigation of Diheme Cytochrome c Peroxidases from Nitrosomonas europaea and Shewanella oneidensis. Biochemistry 2018, 57 (45), 6416–6433. [PubMed: 30335984]
22. Li X; Feng M; Wang Y; Tachikawa H; Davidson VL, Evidence for redox cooperativity between c-type hemes of MauG which is likely coupled to oxygen activation during tryptophan tryptophylquinone biosynthesis. Biochemistry 2006, 45 (3), 821–8. [PubMed: 16411758]
23. Abu Tarboush N. Unraveling the Mechanism and Structural Determinants of Electron Transfer through the Di-heme Enzyme MauG. Ph.D, University of Mississippi Medical Center, Jackson, MS, 2011.
24. Rönnberg M, Lambeir A, Ellfolk N. and Dunford HB, Kinetics of cyanide binding by half-reduced Pseudomonas cytochrome c peroxidase. Biochim. Biophys. Acta 1985, 828, 67–72.

25. Weitz AC; Biswas S; Rizzolo K; Elliott SJ; Bominaar EL; Hendrich MP, The electronic state of the His/Tyr-ligated heme of BthA by Mössbauer and DFT analysis. Inorganic Chemistry, in press.

26. Debrunner, Mossbauer Spectroscopy of Iron Porphyrins. In Iron Porphyrins Part III, Lever ABP; Gray HB, Eds. VCH: New York, 1989; Vol. IV, pp 137–234.

27. Abu Tarboush N; Shin S; Geng J; Liu A; Davidson VL, Effects of the loss of the axial tyrosine ligand of the low-spin heme of MauG on its physical properties and reactivity. FEBS letters 2012, 586 (24), 4339–43. [PubMed: 23127557]

28. Bradley AL; Chobot SE; Arciero DM; Hooper AB; Elliott SJ, A distinctive electrocatalytic response from the cytochrome c peroxidase of nitrosomonas europaea. The Journal of biological chemistry 2004, 279 (14), 13297–300. [PubMed: 14973133]

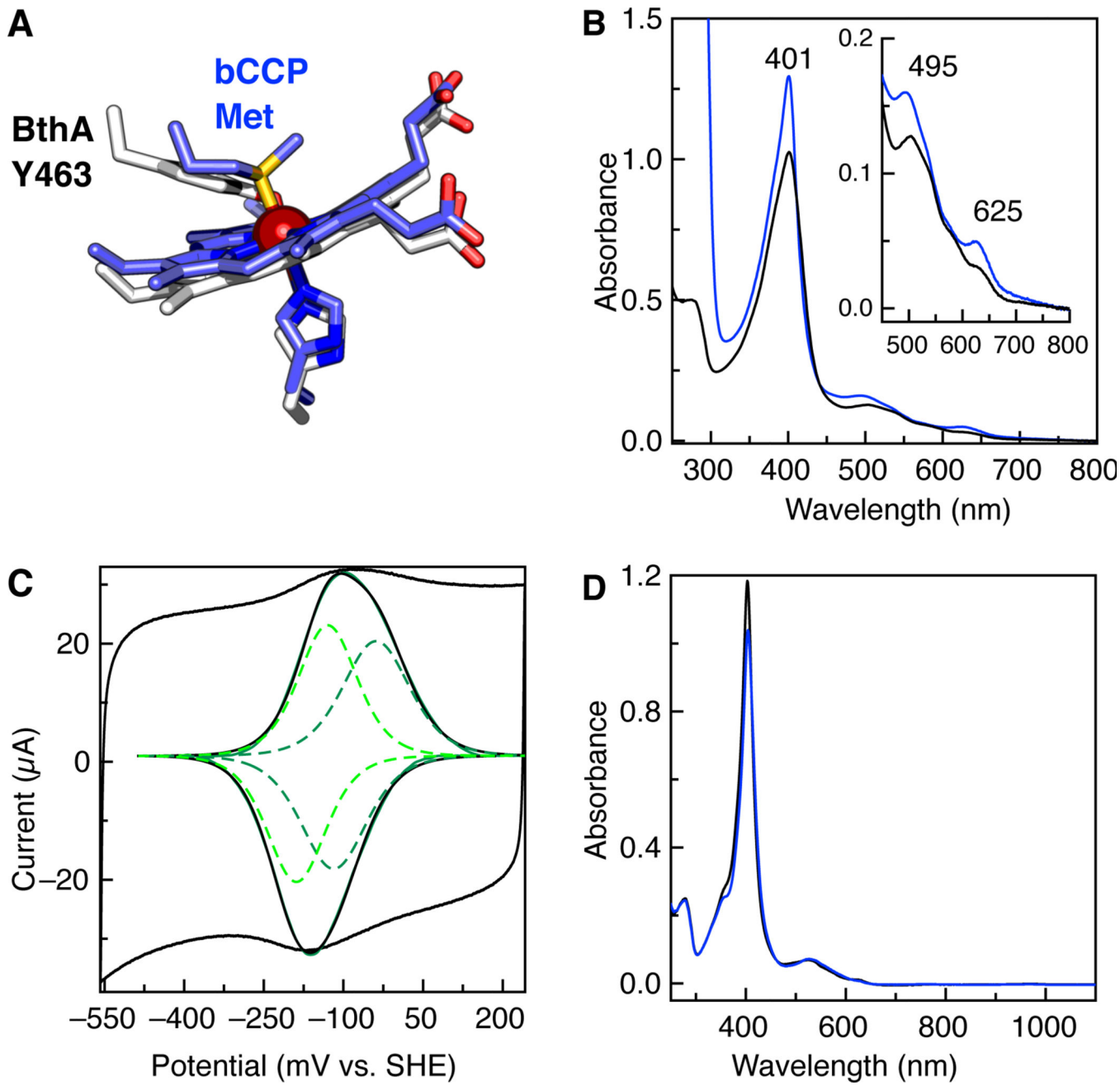

Figure 1.

Biophysical characterization of the BthA Y463M variant. (A) Schematic of the 6c heme coordination of BthA and MauG (white) and bCCPs (slate), comparing BthA (PDB ID 6NX0.pdb) and CcpA from *Shewanella oneidensis* (3O5C.pdb). (B) Absorption spectra of aerobically purified (solid) and ascorbate treated (blue) Y463M BthA. (C) Voltammogram of Y463M at pH 7.3, 21˚C, 50 mV/s. Raw voltammogram is shown (black) with the baseline subtracted (black, inset) with fit for the overall signal (green) and individual species fit (green dotted lines, inset). (D) Spectra of 5 μM as-isolated Y463M (solid black line) and then treated with 10x H_2O_2 (blue)., 50 mM HEPES, pH 7.8.

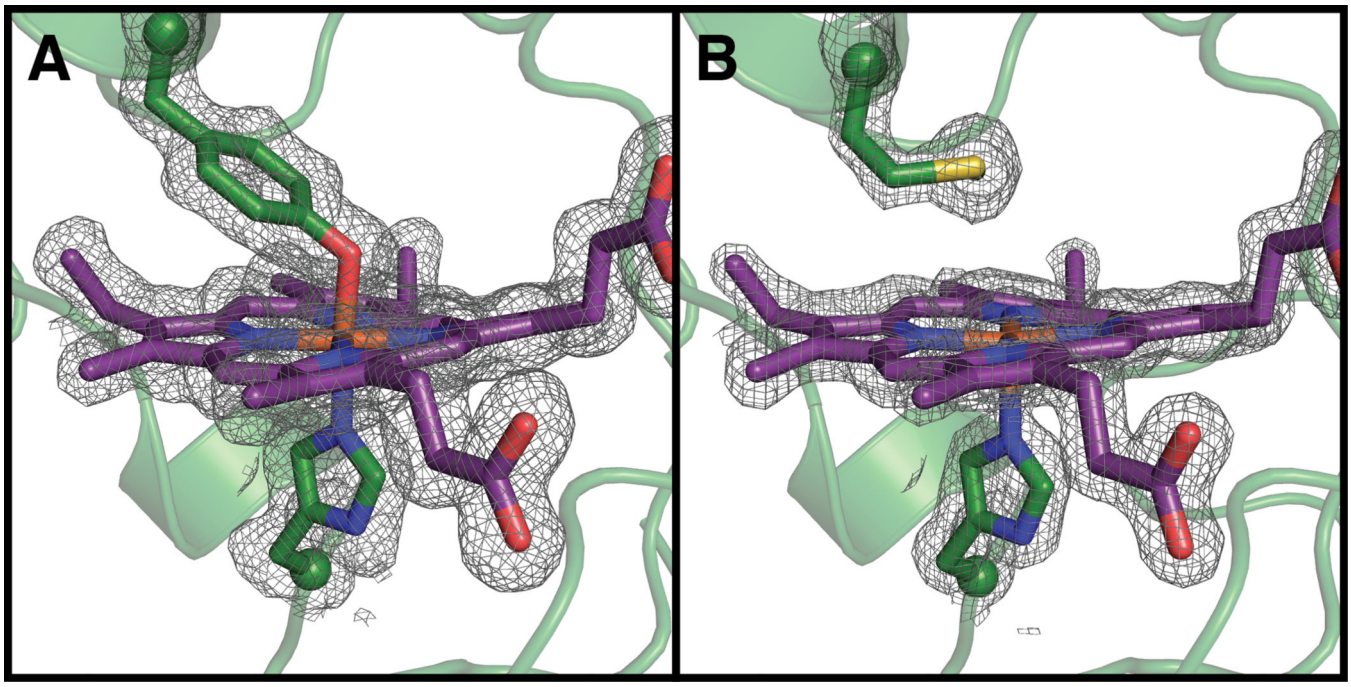

Figure 2.

Compared to the wild-type structure (A; PDB ID: 6NX0), the Y463M mutant (B, PDB ID: 6V59) disrupts axial heme ligation. $2F_O - F_C$ composite omit electron density countoured at 1 σ Peptide and heme carbon shown in green and purple, respectively. Oxygen, nitrogen, sulfur, and iron shown in red, blue, yellow, and orange, respectively. Peptide backbone shown in ribbons representation and side chains and hemes shown in stick representation. Side chain α-carbon shown as spheres. Terminal methyl group of Met side chain is not visible in this orientation. $2F_O - F_C$ electron density shown in grey and contoured at 1σ.

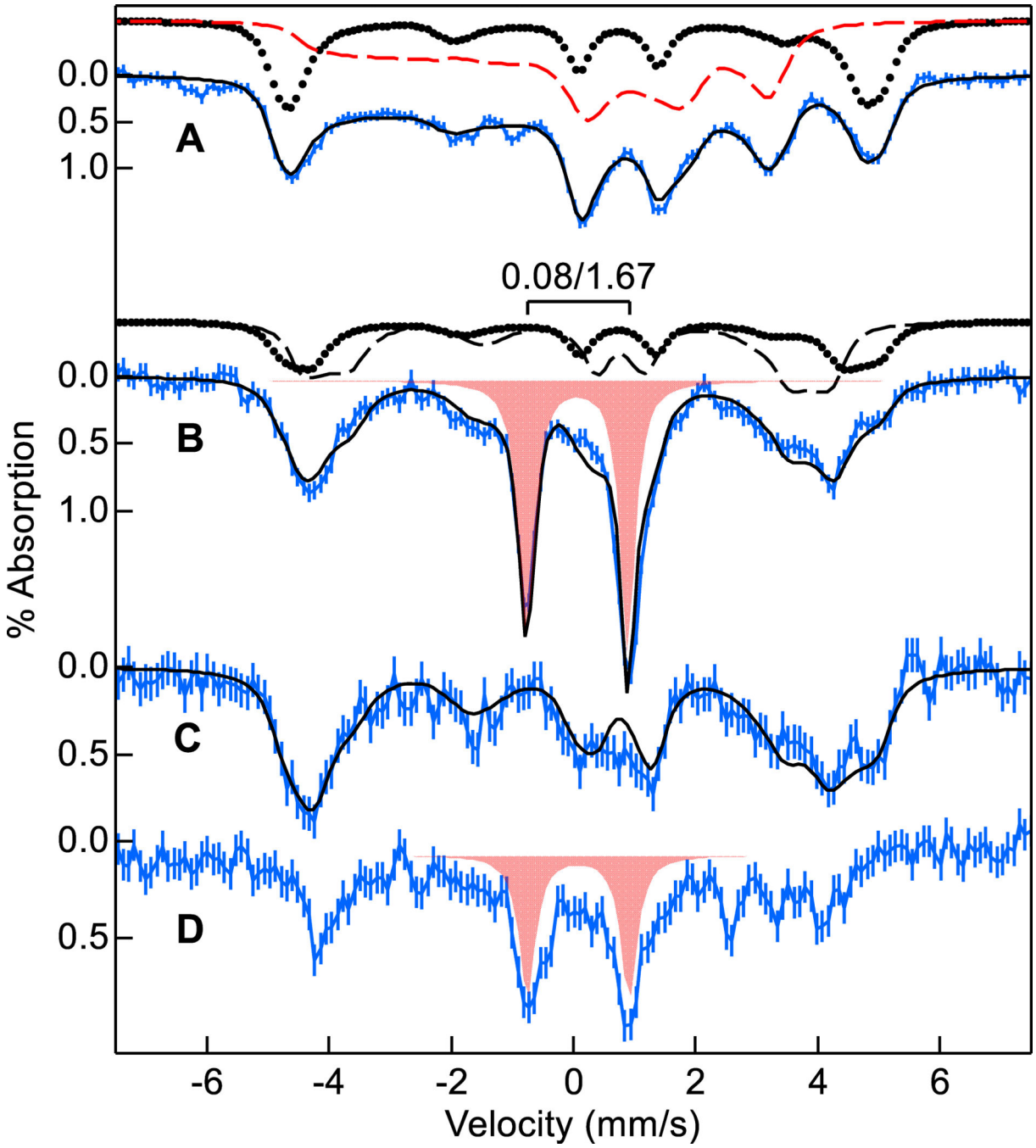

Figure 3.

^{57}Fe enriched Mössbauer spectra (4.2 K, 45 mT, blue vertical bars) of (A) WT BthA and (B) as-isolated BthA Y463M. (C) Y463M plus 30 equiv sodium ascorbate. (D) C, plus 20 equiv of H_2O_2. The black traces overlying the data are simulated sums of species: LS (red dash), HS E/D = 0 (dots), HS E/D = 0.02 (black dash), Fe(IV)=O (red fill). The simulation in C uses the HS species of B, but in larger amounts.

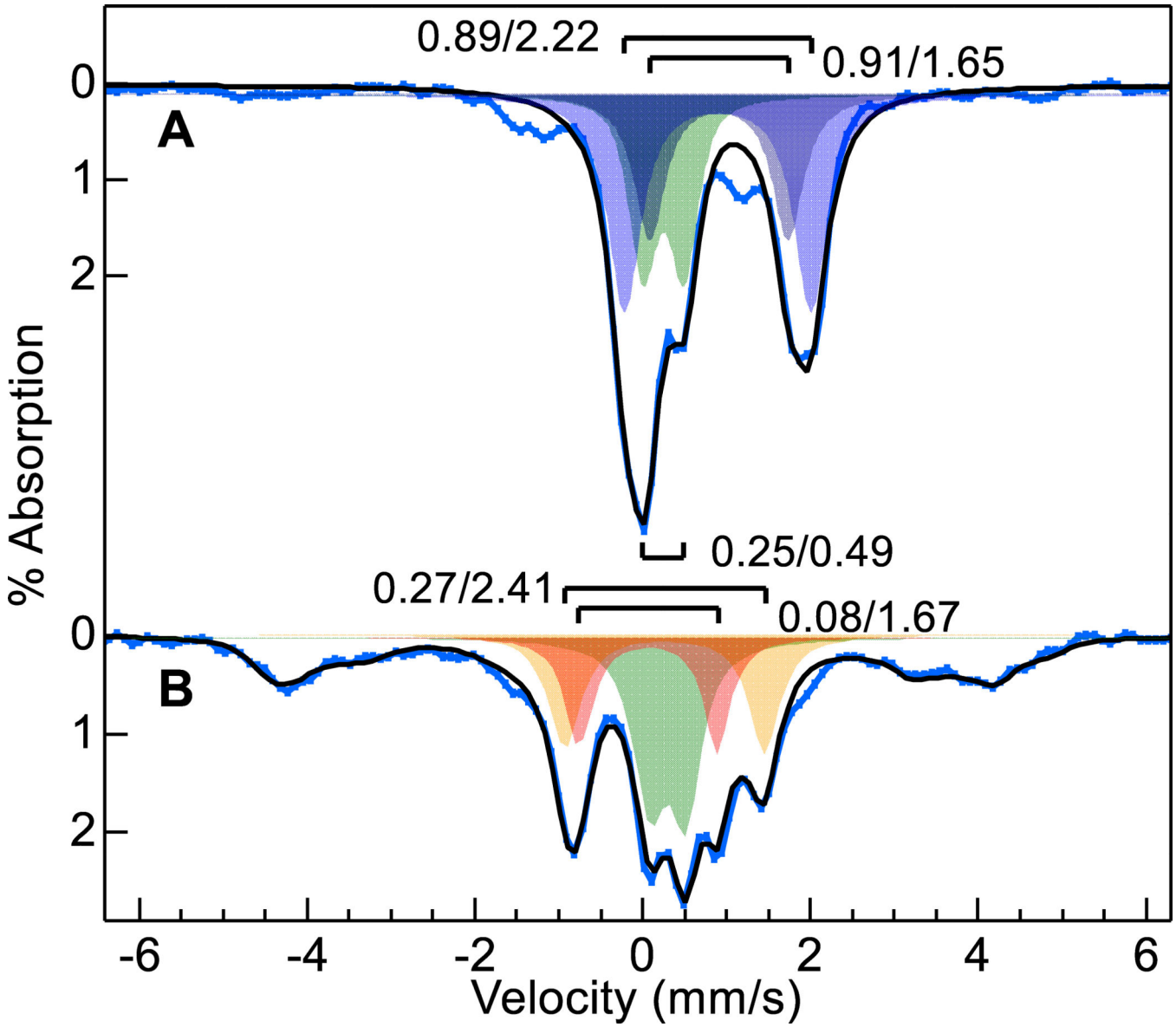

Figure 4.

^{57}Fe enriched Mössbauer spectra (4.2 K, 45 mT, blue vertical bars) of (A) anaerobically purified Y463M BthA, (B) A exposed to O_2 gas for 10 min. The black traces overlying the data are simulated sums using the listed doublet parameters: Fe(II) (blue fill), Fe(II)-CO (green fill), oxy-heme (orange fill), Fe(IV)=O (red fill). The broad magnetic HS species in B are fit with the same species shown in Fig. 3B (black dots and dashed).